Structure, Vol. 13, 905–917, June, 2005, ©2005 Elsevier Ltd All rights reserved. DOI 10.1016/j.str.2005.03.016

Crystal Structure of Human Lectin-like, Oxidized Low-Density Lipoprotein Receptor 1 Ligand Binding Domain and Its Ligand Recognition Mode to OxLDL

Izuru Ohki,[1] Tomoko Ishigaki,[1] Takuji Oyama,[1] Shigeru Matsunaga,[2] Qiuhong Xie,[2] Mayumi Ohnishi-Kameyama,[2] Takashi Murata,[2] Daisuke Tsuchiya,[1] Sachiko Machida,[2] Kousuke Morikawa,[1] and Shin-ichi Tate[1,*]

[1]Department of Structural Biology
Biomolecular Engineering Research Institute 6-2-3
Furuedai
Suita
Osaka, 565-0874
Japan

[2]National Food Research Institute
Tsukuba
Ibaraki, 305-8642
Japan

Summary

Lectin-like, oxidized low-density lipoprotein (LDL) receptor 1, LOX-1, is the major receptor for oxidized LDL (OxLDL) in endothelial cells. We have determined the crystal structure of the ligand binding domain of LOX-1, with a short stalk region connecting the domain to the membrane-spanning region, as a homodimer linked by an interchain disulfide bond. In vivo assays with LOX-1 mutants revealed that the "basic spine," consisting of linearly aligned arginine residues spanning over the dimer surface, is responsible for ligand binding. Single amino acid substitution in the dimer interface caused a severe reduction in LOX-1 binding activity, suggesting that the correct dimer arrangement is crucial for binding to OxLDL. Based on the LDL model structure, possible binding modes of LOX-1 to OxLDL are proposed.

Introduction

Oxidative stress plays a central role in atherogenesis (Kita et al., 2001). Oxidative stress modifies low-density lipoprotein (LDL), and the oxidized LDL (OxLDL), as a marker of the atherosclerosis, induces endothelial dysfunction and injury (Mehta, 2004). Endothelial dysfunction is believed to be a crucial early step in the development of atherosclerosis. Endothelial cells internalize OxLDL by cell surface receptors, as in the process by which macrophage and smooth muscle cells uptake OxLDL by a variety of scavenger receptors, including SR-AI/II, CD36, and SR-BI (Steinbrecher, 1999). These classical scavenger receptors are either absent or found at very low levels on endothelial cells (Mehta, 2004); the endothelial cells possess a specific type of OxLDL receptor. Lectin-like OxLDL receptor 1 (LOX-1) has been identified as a OxLDL receptor primarily in endothelial cells (Sawamura et al., 1997).

LOX-1 expression is upregulated in pathological conditions affecting the vasculature, such as hypertension, diabetes, and atherosclerosis (Chen et al., 2000; Kataoka et al., 1999; Nagase et al., 1997). The expression of LOX-1 affects a variety of gene expression, including adhesion molecules, endothelial constitutive nitric oxide synthetase (eNOS), and monocyte chemoatractant protein-1 (MCP-1) (Li et al., 2002a; Mehta et al., 2001). OxLDL causes apoptosis in human coronary artery endothelial cells (HCAECs) with the associated upregulation of LOX-1 expression (Li et al., 1998). Intriguingly, a specific antisense to LOX-1 mRNA decreased apoptosis (Li and Mehta, 2000). Immunostaining showed that the most prominent expression of LOX-1 was observed in the endothelial cells of atherosclerotic lesions (Chen et al., 2000). These observations indicate that LOX-1 plays a critical role in endothelial dysfunction and injury, leading to initiation and progression of atherosclerosis (Chen et al., 2002; Kita, 1999).

The LOX-1 gene has been mapped to the genetic region known as the NK-gene complex (NKC) (Aoyama et al., 1999), which mainly encodes receptors associated with natural killer cells (NK cells) (Yokoyama and Plougastel, 2003). As with all lectin-like NK cell receptors encoded in the NKC, LOX-1 is a membrane protein with a type II orientation and displays sequence homology to C-type animal lectins, which bind carbohydrates in a Ca^{2+}-dependent manner (Chen et al., 2002; Drickamer, 1999; Zelensky and Gready, 2003). LOX-1, like other NK cell receptors, consists of four domains: a short N-terminal cytoplasmic domain, a single transmembrane domain, a NECK domain or stalk, and a C-type lectin-like domain (CTLD) at the C-terminal end (Figure 1A). The CTLD in LOX-1 has been confirmed experimentally to be a ligand binding domain (Chen et al., 2001; Shi et al., 2001).

In this study, we report the crystal structure of the LOX-1 ligand binding domain. The structure, which includes only a small region of the NECK domain, is the disulfide-linked homodimer that is the form present on the cell surface. This adds the example of a disulfide-linked dimer structure for proteins in group V of the CTLD family, to which hetero- or homodimer-forming, CTLD-containing NK receptors belong (Drickamer, 1999). In vivo functional assays with LOX-1 mutants revealed that the linearly aligned basic residues at the dimer surface are responsible for ligand binding. We refer to this characteristic structural feature as the "basic spine." In addition, single amino acid substitution of the residue W150 at the dimer interface resulted in a more drastic reduction in binding activity than single amino acid changes at the dimer surface. The combination of structural data and mutational analysis demonstrates the importance of the basic spine on the dimer surface in terms of LOX-1 binding activity. Based on the consensus model structure of LDL, the possible role of the basic spine in OxLDL binding is discussed.

Results

Overall Architectures in Two Crystals

We prepared three forms of the extracellular region of LOX-1 (Figure 1A): the whole extracellular domain, in-

*Correspondence: tate@beri.or.jp

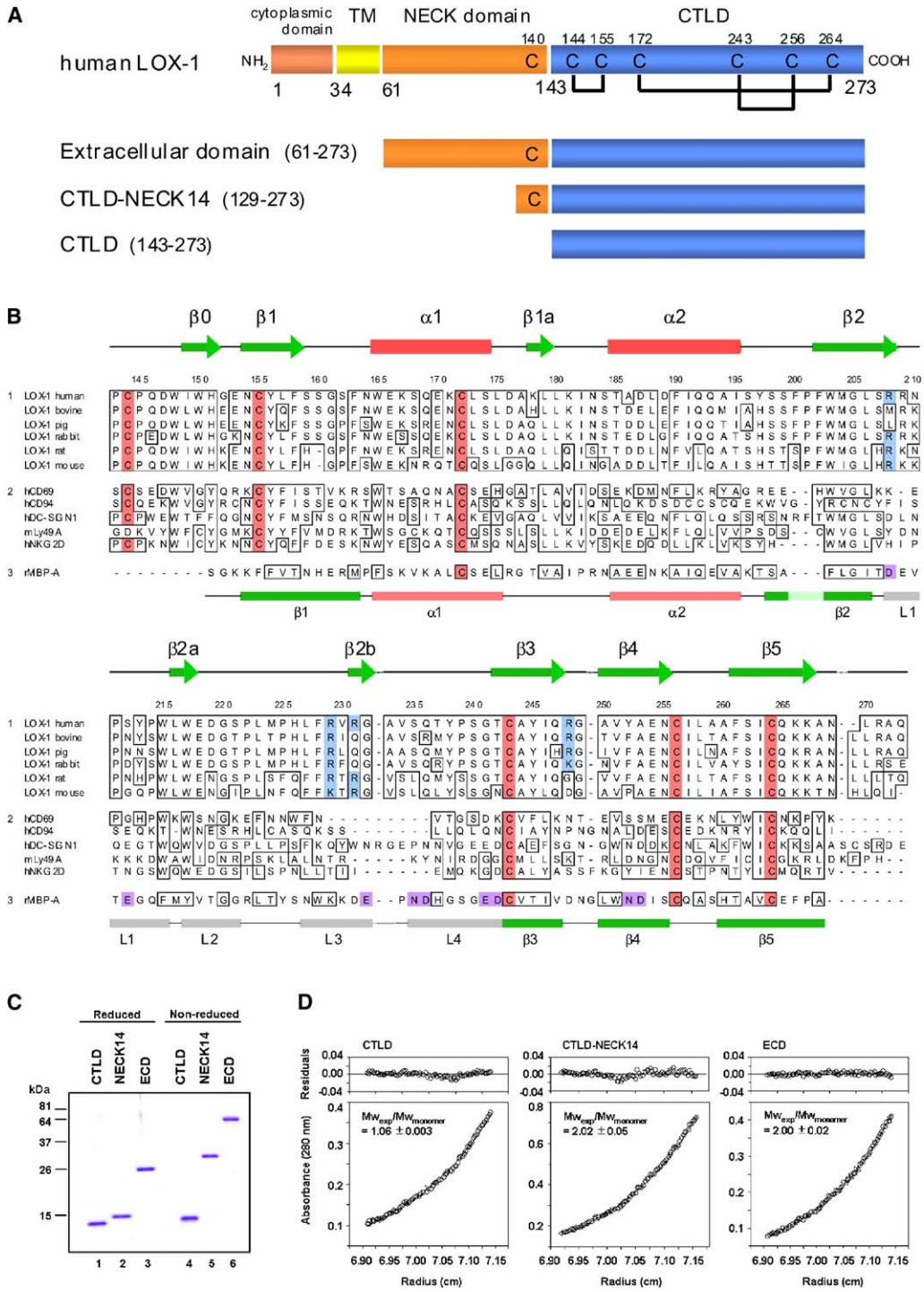

Figure 1. Human LOX-1 Domain Structure and Its Disulfide-Linked Homodimer Formation

(A) Schematic representation of the primary structure of human LOX-1. Four domains are shown by different rectangles: TM, transmembrane domain; CTLD, C-type lectin-like domain. Cysteine residues with intrachain disulfide bonds are highlighted.

(B) Sequence alignment of the CTLDs. The first group contains six LOX-1 orthologs. The second group includes NKDs for natural killer (NK) cell receptors. The sequence of the carbohydrate recognition domain (CRD) of the true C-type lectin MBP-A constitutes group 3. Residues strictly conserved among group 1 are shown in boxes. Homologous residues to LOX-1 CTLD found in the sequences of groups 2 and 3 are boxed. Conserved cysteine residues are marked in red. Basic residues in LOX-1 CTLD, which constitute the basic spine, are marked in blue. The observed secondary structure organization of CTLD in the crystal structure of the LOX-1 disulfide-linked dimer is shown at the top; the green arrow and the red box are the β strand and the α helix, respectively. Secondary structure of rat MBP-A, a canonical CTLD structure, is shown below. The green and red boxes represent the β strand and the α helix, respectively (Weis et al., 1991). The gray boxes in the bottom line represent the loop regions that constitute the long loop region, LLR, commonly found in all CTLDs. The loop numbers denoted as L1–L4

cluding CTDL and the NECK domain (residues 61–273); a fragment of CTLD having a short (14 residue) NECK domain (CTLD-NECK14, residues 129–273); and the CTLD domain only (CTDL, residues 143–273). Each fragment was expressed in *Escherichia coli* and was obtained by in vitro refolding from inclusion bodies.

Two of the recombinant proteins, namely, the whole extracellular domain and CTLD-NECK14, formed homodimers connected by an interchain disulfide bond at C140, as found in the native LOX-1 on the cell surface (Xie et al., 2004). Disulfide bond formation in LOX-1 was confirmed by SDS-PAGE analysis of samples prepared under reduced and nonreduced conditions (Figure 1C). In the absence of the NECK domain, CTLD does not form a stable homodimer in solution, as revealed by analytical ultracentrifugation (Figure 1D). Thus, the NECK domain appears to be essential for maintaining the dimer structure. We crystallized all three LOX-1 fragments. The crystal of the whole extracellular domain did not give good X-ray diffraction data. We then focused on the LOX-1 CTLD and the CTLD-NECK14 fragments in the subsequent structural work.

The CTLD fragment (residues 143–273) was crystallized in an acidic solution consisting of 0.1 M citrate buffer (pH 3.6–3.8). The crystal we obtained belongs to the space group $P2_12_12_1$ with unit cell dimensions of a = 56.79 Å, b = 67.57 Å, and c = 79.02 Å. Two CTLD molecules were in the asymmetric unit (Figure 2A). The structure of CTLD was solved with multiwavelength anomalous diffraction (MAD) by using a SeMet-CTLD and was refined to 1.8 Å resolution (Table 1).

The CTLD-NECK14 crystals were obtained under near physiological conditions (10 mM Tris-HCl [pH 7.5], 400 mM NaCl). These crystals belong to the space group C2 with a = 70.86 Å, b = 49.54 Å, c = 76.73 Å, and β = 98.59°. The structure of CTLD-NECK14 was determined at 2.4 Å resolution by molecular replacement by using the structure of LOX-1 CTLD solved with the above-mentioned CTLD crystal (Table 1).

The LOX-1 CTLD forms a crystallographic dimer. The relative orientation of the subunits in the LOX-1 CTLD dimer is almost inverted compared with that found in the CTLD-NECK14 covalently linked dimer (Figures 2A and 2B). The crystallographic dimer structure for the LOX-1 CTLD shows the interchain parallel arrangement of the most N-terminal β strand, β0, at the dimer interface (Figure 2A). The disulfide-linked CTLD-NECK14 dimer displays a similar arrangement to those commonly found in the crystallographic dimer for the CTLDs of natural killer receptors, which are so called natural killer domains (NKDs) (Figure 2B). In LOX-1 CTLD-NECK14, the β0 strand forms interchain antiparallel β sheets through three hydrogen bonds and two salt bridges, which define the specific relative orientation of the two subunits (Figure 3B). This interconnected β0 strand contains a conserved sequence motif (W-I/L-W-H) among the six LOX-1 orthologs (Figure 1B). A similar motif (W-X-X-Y/F), in which the second residue is hydrophobic, is conserved in the NKDs (Natarajan et al., 2002) (Figure 1B). The interchain disulfide bond in CTLD-NECK14 was chemically confirmed, but there was no interpretable electron density to identify it, suggesting that the short NECK domain in CTLD-NECK14 is intrinsically mobile.

There are different numbers of residues seen in the two independent copies of NECK. The longer NECK is observed from A136, and the shorter one is seen from A141. The longer NECK is more visible because of crystal contact. Both copies in the CTLD-NECK14 covalent dimer structure were visible up to L270.

The LOX-1 CTLD Fold

As predicted by amino acid sequence similarity, the LOX-1 ligand binding domain displays the salient features of the CTLD fold (Figure 2C). There are two types of CTLD structure with significant differences in the orientation of the second α helix, α2. Ly49A, as a representative structure in the atypical class, shows a different α2 orientation from that found in a canonical CTLD structure of MBP-A (Figure 2C). The superposition of LOX-1 CTLD onto Ly49A results in a 1.2 Å root mean square (rms) deviation for 92 Cα pairs. LOX-1 CTLD thus belongs to the rare type of the CTLD fold represented by Ly49A (Figure 2C).

LOX-1 CTLD contains all of the main secondary structure elements found in other members of the C-type lectin-like superfamily (Figure 2B). Strand β2 forms a short β hairpin with the β2a strand. There is an additional parallel β sheet located between β2b and β4 (Figure 2B). The upper part of the molecule is characterized by a segment of polypeptide, located between strands β2a and β2b, that lacks regular secondary structure. This connecting region is called the long loop region (LLR), a variable segment involved in specific ligand binding for each CTLD (Zelensky and Gready, 2003). Like NKDs, the LLR structure in LOX-1 CTLD differs substantially from the corresponding region in the canonical C-type lectins in that it lacks the Ca^{2+} binding site that is critical for carbohydrate recognition domains (CRD) (Figure 2C). In fact, LOX-1 does not require Ca^{2+} for its ligand binding. A notable structural feature of LOX-1 is that both ends of the LLR are fixed by antiparallel (β2–β2a) and parallel (β2b–β4) β sheets (Figure 2B).

One copy of the CTLD-NECK14 structure contacts the molecule in the neighboring crystal unit. Using 128

are defined from the crystal structure of rat MBP-A (Weis et al., 1991). Residues in purple boxes in the MBP-A sequence coordinate the Ca^{2+} ion required in carbohydrate binding.

(C) SDS-PAGE of refolded LOX-1 proteins. CTLD, NECK14, and ECD denote truncated recombinant versions of LOX-1, CTLD (142–273), CTLD-NECK14 (129–273), and the whole extracellular domain (61–273), respectively. The samples treated with β-mercaptoethanol to cleave the disulfide bonds were run in the lanes denoted as "reduced." Lanes shown as "nonreduced" indicate samples in which the disulfide bonds were retained.

(D) The results of the analytical ultracentrifugation for the LOX-1 proteins; CTLD, CTLD-NECK14, and the whole extracellular domain (ECD). Curve fitting to the experimental data with a single component model and the residuals of the observed data from the fit model curve are shown. The number of subunits in a molecule determined by the analysis is shown in each sedimentation profile.

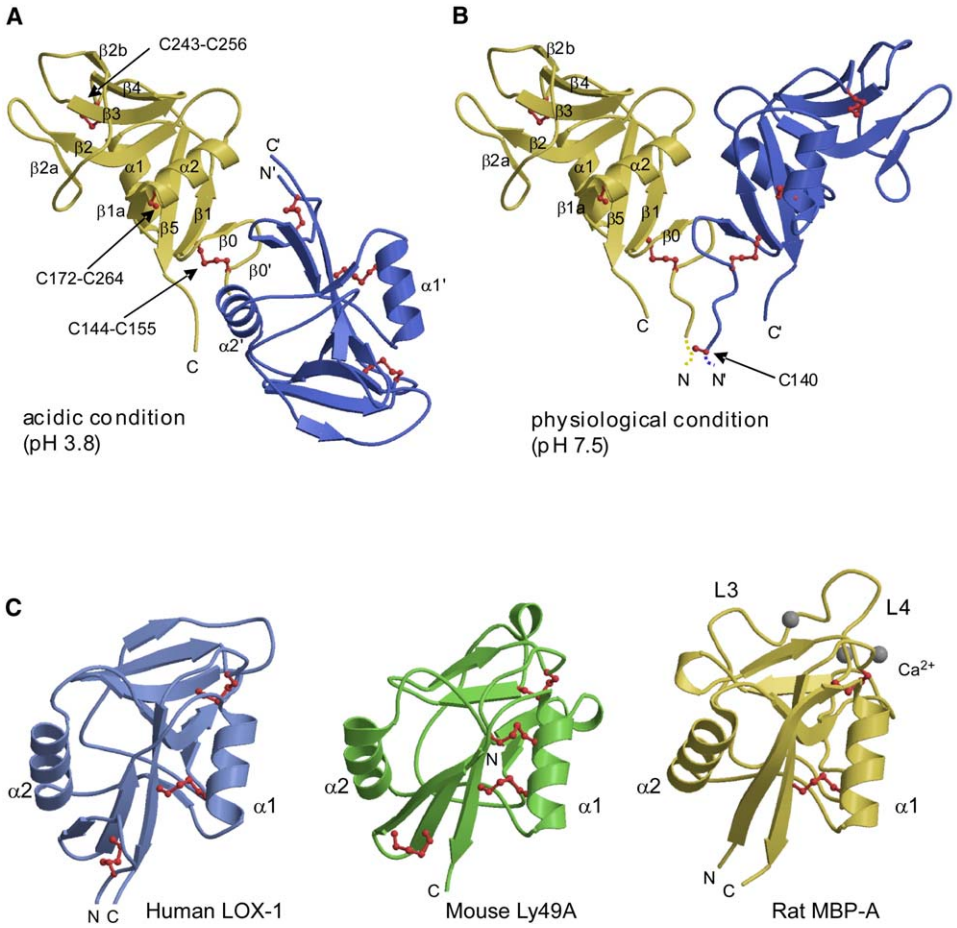

Figure 2. Two Crystal Forms of LOX-1 and the Structural Comparison of the CTLD with Other Members of the C-Type Lectin-like Family

(A) Structure of the crystallographic dimer of LOX-1 CTLD (143–273). The crystal was obtained from acidic solution. Two molecules in a unit cell are shown as a different color. The secondary structures are denoted by the symbols defined in Figure 1B. The intrachain disulfide bonds are shown by red balls-and-sticks.

(B) Structure of the LOX-1 CTLD-NECK14 (129–273), which is in the disulfide-linked dimer form. Each subunit in the dimer is shown in a different color. Due to the structural flexibility of the N-terminal region, only one C140 was observed in the electron density map. The possible interchain disulfide bond is shown by red ball-and-stick representation.

(C) Structure of LOX-1 CTLD and comparison with other members of the C-type lectin-like family. Ribbon diagrams of the LOX-1 CTLD (left), Ly49A (center), and MBP-A (right) are shown in a common orientation. The Ca^{2+} ions bound to MBP-A are shown as gray spheres. The loops in the long loop region, LLR, involved in Ca^{2+} coordination are labeled in the structure of MBP-A. Two α helices in the CTLDs are labeled as α1 and α2. In both LOX-1 and Ly49A, the α2 helix is rotated by about 20°, as compared with MBP-A and most other members of the C-type lectin-like family. Disulfide bonds in each CTLD are shown by red ball-and-stick representation. PDB codes for Ly49A and MBP-A are 1QO3 (Tormo et al., 1999) and 2MSB (Weis et al., 1992), respectively. Secondary structure elements were defined by using procedures in MOLMOL according to the Kabsch/Sander algorithm (Koradi et al., 1996). All figures were prepared by the program MOLSCRIPT (Kraulis, 1991).

Cα carbons in residues 143–270 (Figure S1; see the Supplemental Data available with this article online), we showed that superposition of a copy of CTLD-NECK14 that does not show the crystal contact with a copy in the LOX-1 CTLD crystallographic dimer showed 0.5 Å rms deviation. The corresponding value for the other copy of CTLD-NECK14 having the crystal contact was 1.2 Å. We concluded that the monomer unit of the LOX-1 ligand binding domain retains essentially the same structure in the different crystal conditions. Therefore, the LLR forms a specific conformation, despite the lack of any regular secondary structure.

The LOX-1 CTLD-NECK14 and the CTLD crystals were obtained under neutral and acidic pH conditions, respectively. The above-mentioned structural comparisons may also mean that solution pH differences do not alter the ligand binding domain structure of LOX-1. This suggests that the LOX-1 ligand binding domain retains its structure in the endosome where the pH is in the acidic range (<pH 6) (Murphy et al., 1984). Although each ligand binding domain per se does not show significant structural change, we cannot rule out the possibility of pH-induced dimer disarrangement in LOX-1. Such a change is inferred from the different dimer arrangements found in the two crystal structures (Figures 2A and 2B). The possible dimer disarrangement of LOX-1 may be related to the proposed structural change of the LDL receptor, which is believed to be

Table 1. Data Collection and Crystallographic Refinement

		CTLD (Acidic Condition)			
Data Collection[a]	CTLD-NECK14	SeMet1	SeMet2 (Peak)	SeMet2 (Rdge)	SeMet2 (Temote)
Wavelength (Å)	1.0000	1.0000	0.9792	0.9794	0.9762
Resolution (Å)	37.9–2.40	50.0–1.78	50.0–1.96	50.0–1.96	50.0–1.96
Unique reflections	10,449	33,424	25,180	25,265	25,653
Completeness (%)	99.3 (99.3)	99.6 (99.7)	100.0 (99.9)	100.0 (99.9)	100.0 (99.9)
R_{merge} (I)[b] (%)	8.1 (36.4)	5.3 (39.5)	7.1 (22.7)	6.4 (25.2)	6.2 (22.6)
MAD Phasing					
Number of sites			6	6	6
Phasing power[c] (centric/acentric)			1.43/1.09	1.32/0.58	0.00/1.07
Figure of merit[d] (centric/acentric)			0.80/0.77		
Structure Refinement	CTLD-NECK14	CTLD (SeMet1)	CTLD (SeMet2)		
Resolution (Å)	37.0–2.40	30.0–1.78	30.0–1.96		
Reflections (cryst/free)	9,824/546	30,428/1,597	23,656/1,230		
Protein/solvent atoms	2,111/52	2,292/215	2,264/177		
R_{cryst}/R_{free}[e] (%)	20.0/27.5	20.9/23.0	20.8/24.4		
Rmsd (bond/angle)	0.009 Å/1.4°	0.005 Å/1.2°	0.005 Å/1.2°		

[a] Values in parentheses indicate statistics for the last shell.
[b] $R_{merge} = \Sigma_i\Sigma_j|\langle I_j\rangle - I_{ij}|/\Sigma_i\Sigma_j I_{ij}$, where $\langle I_i\rangle$ is the mean intensity of the ith unique reflection, and I_{ij} is the intensity of the jth observation.
[c] Phasing power = <F(H)>/E, where <F(H)> is the rms amplitude of the heavy atom structure factor, and E is the residual lack of closure error.
[d] Figure of merit = $\langle\Sigma P(\alpha)\exp(i\alpha)/\Sigma P(a)\rangle$, where $P(\alpha)$ is the phase probability at the angle α.
[e] R_{free} was calculated by using 5% of total reflections, which were chosen randomly and omitted from the refinement.

induced by exposure to the endosomal pH (Rudenko et al., 2002).

LOX-1 ligand binding domain has three intrachain disulfide bonds (Figure 2B), two of which (C172–C254 and C243–C256) are characteristically invariant disulfide bonds found in all members of the C-type lectin-like domains (Figure 1B). The third disulfide bond is located at C144–C155, which maintains the short antiparallel β sheet between β0 and β1. This short antiparallel β sheet is connected by four hydrogen bonds among backbone atoms (Figure 3A). In addition, W150 Nε1 is hydrogen bonded to the carbonyl oxygen of G152 in the same chain (Figure 3A). This side chain-backbone hydrogen bond contributes to maintaining the proper orientation of W150 and H151. These residues subsequently form interchain hydrogen bonds and salt bridges, which define the specific dimer arrangement (Figure 3B).

In all C-type lectin-like domain structures, the N and C termini are spatially closed (Drickamer, 1999). In LOX-1 CTLD, C155 in the β1 strand is hydrogen bonded to K266 located in the β5 strand, which maintains the N and C termini in spatial proximity (Figure 3A). The antiparallel β sheet between β1 and β5 constitutes the proper overall CTLD fold. Homologous sequences are found in the C-terminal region of all six LOX-1 orthologs (Figure 1B). Machida and coworkers have shown that the deletion of seven residues, KANLRAQ (267–273), from the C terminus of human LOX-1 leads to improper folding within the cell, as revealed by the altered N-glycosylation pattern of the expressed protein (Shi et al., 2001). Deletion of nine residues QKKANLRAQ (265–273) from the C terminus destroyed the structure, and the expressed protein was not present on the cell surface (Shi et al., 2001). These results suggest that the C-terminal homologous region is essential for maintaining the active CTLD fold. This is consistent with the LOX-1 ligand binding domain structure, in which the hydrogen bond between C155-K266 maintains the conserved antiparallel β sheets between β1 and β5. Weakening the C155-K266 hydrogen bond, by deletion of the neighboring C-terminal sequence KANLRAQ (residues 267–273), or eliminating it by deletion of QKKANLRAQ (residues 265–273), results in improper folding of the LOX-1 ligand binding domain.

The LOX-1 CTLD Homodimer

Human LOX-1 exists as a disulfide-linked homodimer at C140 on cell surfaces (Xie et al., 2004). The formation of a disulfide-linked dimer is the common structural feature in the C-type lectin-like NK receptors (Natarajan et al., 2002). Unlike C-type lectin-like NK receptors, this interchain disulfide bond is not conserved among other LOX-1 orthologs. In addition, this interchain linking does not seem to be essential for the recognition of modified LDL by human LOX-1. The C140S mutation of human LOX-1 retained the ability to bind modified LDL, although it showed reduced binding to bacteria (Xie et al., 2004).

The high level of sequence similarity of the NECK to a myosin heavy chain suggests that the LOX-1 NECK should form a parallel coiled-coil structure as in the myosin tail (Lupas, 1996). The presumed overall structure for the complete extracellular domain of LOX-1 is shown schematically (Figure 3C). Secondary structure predictions suggest, however, that the α-helical region may not extend through the entire NECK domain, there being a break at the center of the NECK domain. This break would confer a flexible arrangement for the C-terminal ligand binding domains on the cell surface. Intriguingly, this predicted helix break is close to the cleavage site for generating a soluble form of LOX-1, mediated by an unknown protease on the cell surface (Murase et al., 2000).

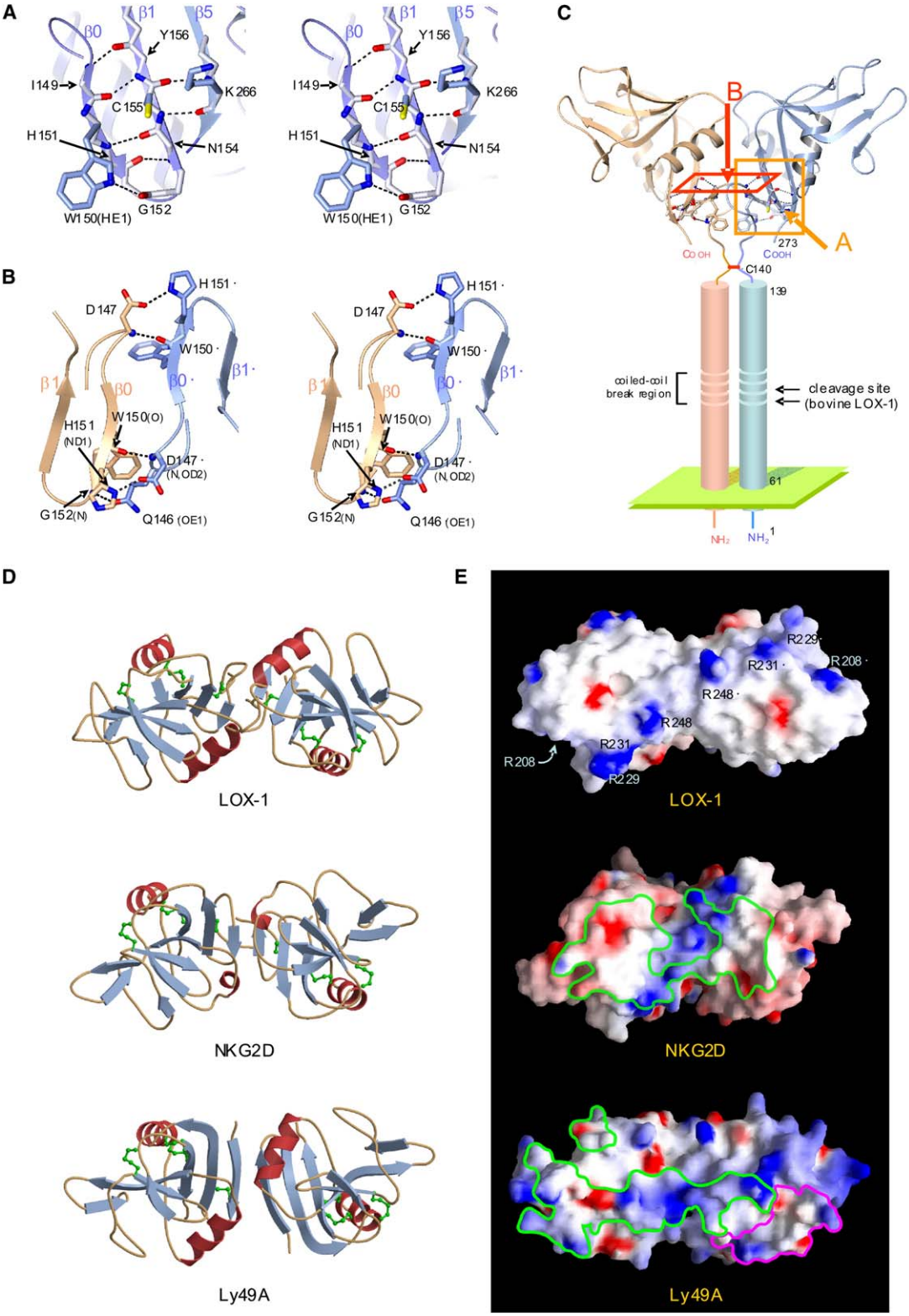

Figure 3. Hydrogen Bonding Network in LOX-1 and Its Dimer Surface Structure

(A) Intrachain hydrogen bonding network in the LOX-1 CTLD.

(B) Hydrogen bonds connecting the two subunits of the LOX-1 CTLD dimer.

(C) Schematic drawing of the entire architecture of LOX-1. The C-terminal dimer CTLD is the crystal structure determined in this work. The NECK domain, residues 61–139, is drawn as a coiled-coil structure predicted according to its sequence characteristics. In this figure, a possible break in the coiled-coil structure and the N-terminal cleavage positions to generate the soluble form of LOX-1, which were deter-

The LOX-1 CTLD per se does not form a stable homodimer (Figure 1D). The crystal structure of CTLD-NECK14 has shown that the interchain disulfide bond helps the proper dimer formation of the LOX-1 CTLDs. In other LOX-1 orthologs, the CTLD dimer arrangement is defined by the coiled-coiled structure formed in the NECK domain, which functionally compensates for the loss of the interchain disulfide bond. This also explains the minimal impact on function upon loss of the interchain disulfide bond in human LOX-1 (Xie et al., 2004).

The Ligand Binding Surface of LOX-1—Basic Spine Structure

The dimer surface contains the most variable part of CTLD, the LLR, in terms of structure and amino acid sequence. This variability explains the importance of this part of the molecule in selective ligand recognition. In Ly49A, this region contains the binding site for its ligand, MHC class I molecules (Tormo et al., 1999). The corresponding region in NKG2D is also known to be important for ligand binding (Li et al., 2001, 2002b; McFarland et al., 2003; Radaev et al., 2001). The binding surfaces for NKG2D and Ly49A are well characterized in their complex structures with ligands. The binding regions are marked on their surface charge maps (Figure 3E). Each NKD uses the particular surface area to enable specific ligand recognition.

Sequence and structural comparisons of the C-type lectin-like family proteins revealed that the LLR plays a homologous role to that of the hypervariable loop of the immuoglobulin domain (Zelensky and Gready, 2003). The LLR is, thus, a structurally independent part of CTLD, suggesting that the LLR is a flexible unit for adaptive evolution (Zelensky and Gready, 2003). The observed diversity in the dimer surface structure can be ascribed to sequence variation in the LLR (Figure 1B).

The characteristic LLR sequence of LOX-1 gives a distinctive charge distribution at the ligand binding surface. There is a linear arrangement of basic residues crossing over the dimer surface of LOX-1, which we call the "basic spine" (Figure 3E). Arginine residues in the LLR and R248 form the basic spine (Figures 1B and 3E). Acidic spots, arising from E254 in each subunit, are also present, although these do not appear to influence binding activity (Shi et al., 2001) (Figure 3E). By contrast with other NKDs, the LOX-1 dimer surface is primarily hydrophobic (Figure 3E). LOX-1 preferentially binds to negatively charged molecules, including OxLDL, the apoptotic cell whose surface is rich in negatively charged phosphatidyl serine moieties, and poly anion molecules like poly inosinic acids (Chen et al., 2002). The basic spine appears to be responsible for specific ligand recognition.

Role of the Residues in the Basic Spine

We explored the biological significance of the basic spine on the LOX-1 dimer surface by introducing single amino acid substitutions.

The ability of LOX-1 mutants to take up acetylated LDL (AcLDL) into living cells was assayed by microscopic observation (Figure 4). AcLDL was used as an alternative ligand to OxLDL, which shows comparable affinity to LOX-1 (Shi et al., 2001), in order to avoid ambiguous effects from variations in the extent of OxLDL oxidation (Lougheed and Steinbrecher, 1996; Yoshida et al., 1998). In this assay, the amount of incorporated AcLDL directly reflected the binding activity of LOX-1, which was confirmed by independent analysis as described previously (Chen et al., 2001). The mutants R208N, R229N, and R248N were expressed normally on the cell surface but showed reduced AcLDL uptake, thus showing their reduced binding activities. R231N displayed no detectable AcLDL binding activity. As a control, H226A, which is located outside the basic spine, showed no reduction in binding activity. Each Arg residue in the basic spine plays a significant role in LOX-1 ligand binding (Figure 3E). Interestingly, R209N had little effect on the binding activity, although the R208N was effective (Figure 4). This is because R209 is located beneath the binding surface.

Except for R231N, single amino acid changes in the basic spine showed only a moderate effect on ligand binding. This binding feature is consistent with that for the scavenger receptor, SR-A. In the case of SR-A, the substitution of more than two lysine residues in a conserved basic amino acid cluster in the collagen-like domain was required to abolish the binding to OxLDL (Doi et al., 1993).

Mutation of a Residue at the Homodimer Interface

Our mutant analyses show that residue W150, located at the dimer interface, plays a major role in the LOX-1 binding activity. The mutation W150A results in an almost complete loss of binding activity to AcLDL (Figure 4). Except for R231, this result contrasts with the moderate effect of single amino acid changes to the basic spine. The LOX-1 dimer structure shows that the W150 contributes not only to dimer formation but also to maintaining the proper CTLD fold through inter- and intrachain hydrogen bonds (Figures 3A and 3B). Loss of the W150 side chain to the G152 backbone hydrogen bond should deform the β0 strand that makes the interchain antiparallel β sheet (Figure 3B). Because the interchain hydrogen bonds define the specific orientation of the two subunits of dimer, disturbance of this hydrogen bond network may induce dimer disarrangement. In turn, this will disrupt the basic spine structure

mined for bovine LOX-1 (Murase et al., 2000), is shown. Two boxes on the CTLD crystal structure indicate the view positions for (A) and (B).
(D) Ribbon representation of the CTLD dimer structures for LOX-1, NKG2D, and Ly49A. The latter two dimers are the crystallographic dimers without covalent linkage.
(E) The surface charge distribution on the dimer surface with the corresponding views of the dimer structures shown in the ribbon representation. Contact area found for NKD2D-MICA (PDB code: 1HYR) (Li et al., 2001) and Ly49A-H-2D (PDB code: 1QO3) (Tormo et al., 1999) complex structures are drawn on their surfaces with green lines. Another contact region in the Ly49A structure in the complex with H-2D^d is drawn with a red line. The contact areas for NKG2D and Ly49A were identified with the maximum distance range for contacting atoms 4.5 Å by the program GRASP (Nicholls et al., 1991). All surface colors drawn on the solvent accessible surface represent $-10\ k_BT^{-1}$ (red) to $+10k_BT^{-1}$ (blue) by using the program GRASP (Nicholls et al., 1991).

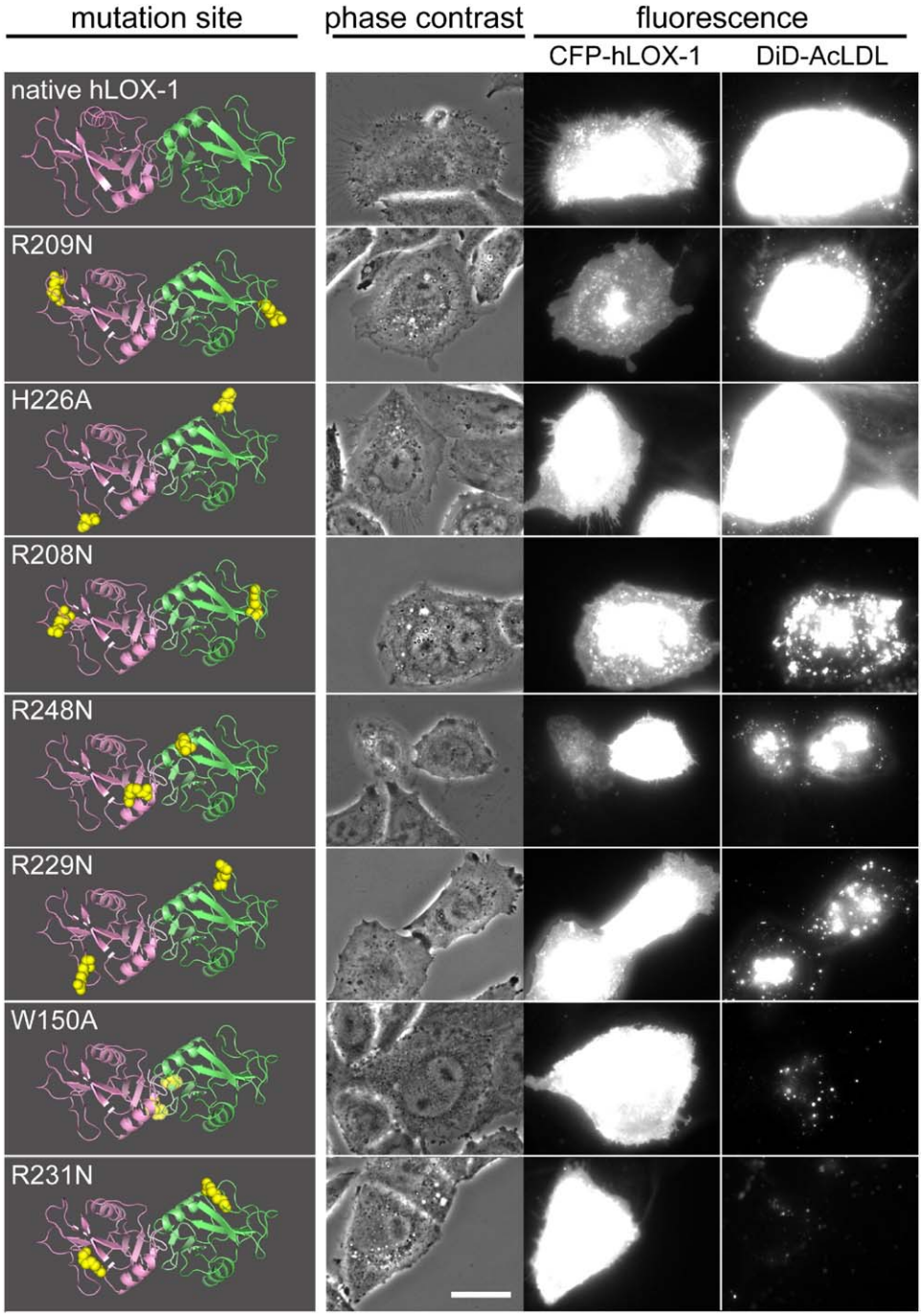

Figure 4. Effect of Amino Acid Substitutions in Human LOX-1 on Ligand Uptake

In the left column, the substituted amino acids are shown by yellow sphere representation on the crystal structure of the CTLD-NECK14 dimer. Phase contrast images of the cells are shown in the second column. The bar in the bottom panel indicates a length of 20 μm. The two columns to the right show the corresponding fluorescence image of the cells in the same view as that used for the phase contrast micrograph. The fluorescence images for CFP-LOX-1 (excitation 436 nm) and DiD-AcLDL (excitation 620 nm) are shown in the left and right panel, respectively.

on the ligand binding surface, which should result in a severe reduction of LOX-1 ligand binding activity.

There is a small, empty cavity in the LOX-1 dimer interface. The cavity, 114 $Å^3$ in volume, is formed by hydrophobic residues, including P143, C144, P145, W148, I149, and W150 (Figure 5A). Although the biological role of this cavity is not immediately apparent, the cavity-forming residues are conserved among all LOX-1 orthologs, with the exception of I149, which is sometimes replaced by leucine (Figure 1B). Substitu-

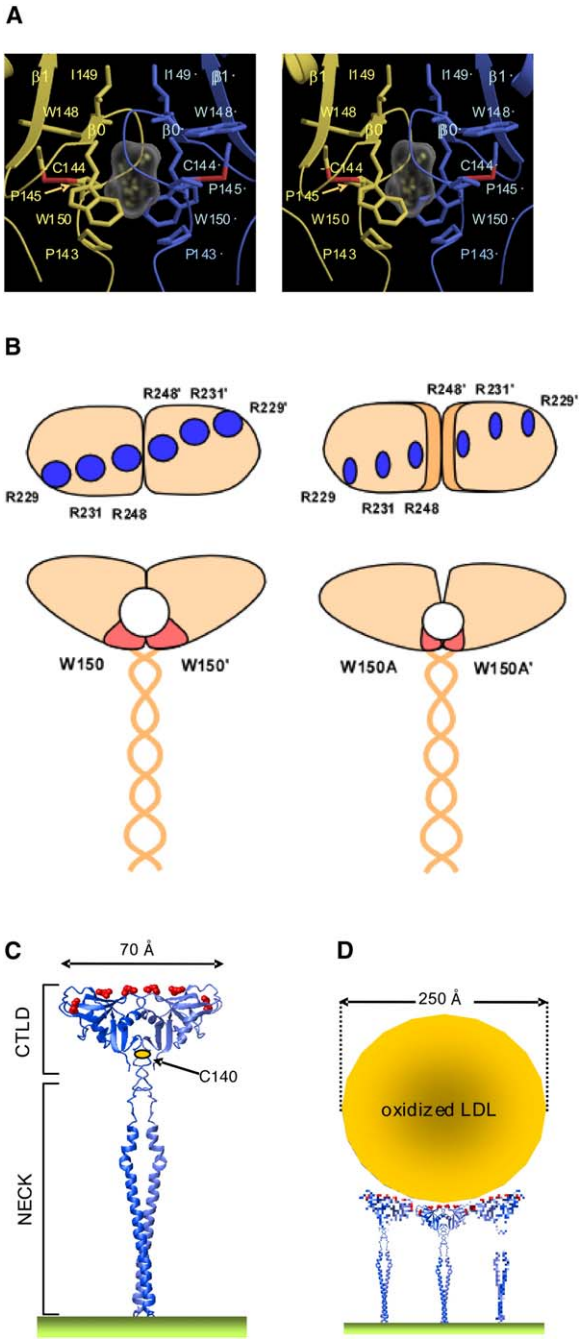

Figure 5. The Empty Cavity in the Dimer Interface of LOX-1

(A) Empty cavity located at the dimer interface in the LOX-1 disulfide-lined dimer structure. The surrounding residues of the cavity are shown as bold lines.

(B) Possible effect of the W150A mutation on the basic spine structure on the LOX-1 ligand recognition surface. The W150A mutation may resize the empty cavity in the dimer interface, which subsequently disarranges the dimer, resulting in the disruption of the basic spine structure. The disrupted basic spine structure should lead to severe reduction of the binding ability to ligands.

(C) A plausible representation of the entire structure of LOX-1 at the cell surface, based on the crystal structure for CTLD and the model structure for the NECK. Modeling was performed by using the myosin heavy chain coiled-coil structure, which shows a high level of sequence homology to the NECK region.

tion of W150, which is located at the bottom corner of the empty cavity (Figure 5A), with an alanine residue may lead to disarrangement of the dimer subunits by closing the bottom of the empty cavity. This possible disarrangement of the dimer, induced by cavity resizing, also facilitates the disruption of the basic spine on the binding surface. Indeed, this could explain the severe reduction of binding activity of the W150A mutant for OxLDL (Figure 5B).

Discussion

Basic Spine Structure for the Ligand Recognition

The structural data presented in this paper show that LOX-1 possesses a basic spine structure across its ligand recognition surface that is predicted to play an essential role in OxLDL binding. There is a paucity of structural data for LDL, which consists of lipids and apolipoprotein B-100 (apoB-100), a single polypeptide comprising about 4,500 residues that wraps the lipid particle. The consensus model reveals that apoB-100 has a pentapartite domain structure, NH_3-βα1-β1-α2-β2-α3-COOH. The α and β domains are mainly composed of amphipathic α helices and β sheets, respectively (Segrest et al., 2001) (Figure S2A). The βα1 domain is thought to be a globular domain, based on homology to lipovitellin (Segrest et al., 2001). The amphipathic β1 and β2 domains display sequence characteristics typical for that of irreversible lipid association (Segrest et al., 2001). However, the α2 and α3 domains show similar sequence properties to that of an exchangeable apolipoprotein, such as apoA-I and apoE, and are assumed to be flexible domains with reversible lipid affinity (Segrest et al., 2001). From the size of the surface area of LDL, the approximate number of amphipathic α helices has been estimated to range from 51 to 65 according to the LDL subclasses (Segrest et al., 2001), suggesting that LDL has amphipathic α helices on its surface (Figure S2B). The basic spine structure provides an appropriate platform for interaction with the α helix in which at least 37 residues are required for full contact (Figure 6A). Thus, we envisage that LOX-1 preferentially binds to an amphipathic α helix on the LDL surface.

LOX-1 assembles on the cell surface as at least a hexamer that comprises three homodimeric LOX-1 molecules in binding to OxLDL (Xie et al., 2004). Comparing the size of the dimer surface of LOX-1 with the diameter of LDL, it seems reasonable that LOX-1 binds to the OxLDL as an assembly (Figures 5C and 5D). The amphipathic α helices on LDL can act as multiple binding sites for LOX-1 assembly on the cell surface.

During oxidation of LDL, there is a progressive de-

(D) Scale comparison between the the OxLDL particle and LOX-1 dimer. The assembled structure of LOX-1 is drawn according to the results of cell biology studies that showed LOX-1 to exist as a hexamer on the cell surface (Xie et al., 2004). The diameter of OxLDL was estimated from cryoelectron microscopic observation of the LDL particle (Segrest et al., 2001). In this comparison, it is assumed that no significant structural alterations are induced by oxidation to the LDL particle.

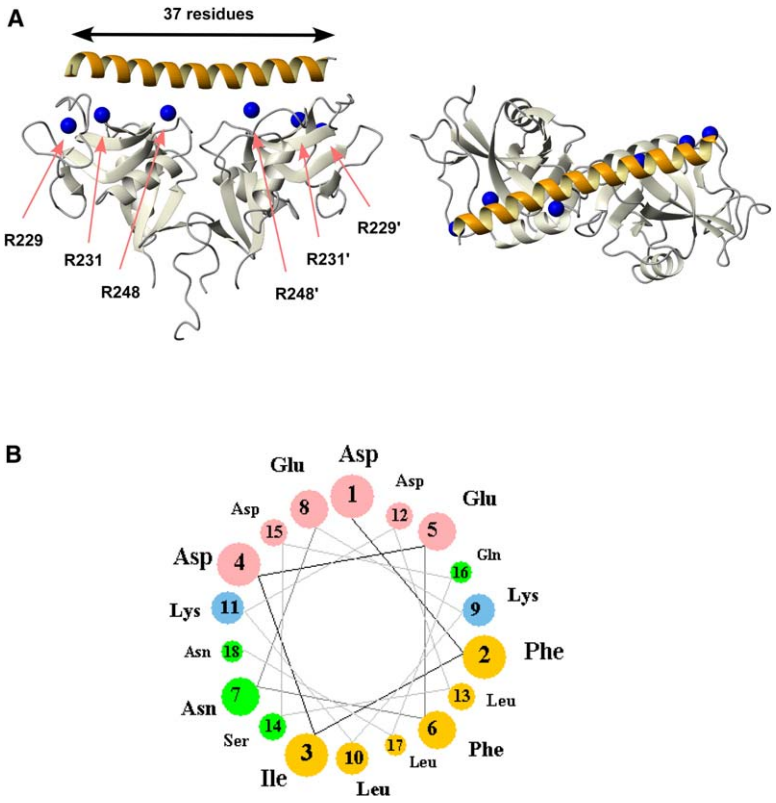

Figure 6. Possible Binding Mode of LOX-1 to apoB-100 in LDL

(A) A model complex structure between the LOX-1 dimer ligand recognition domain and an α helix. The Nε atoms of the arginine residues in the basic spine are drawn with blue spheres. The right figure is drawn from the view rotated by 90° to that of the left figure.

(B) A helical-wheel presentation of the 22 residue consensus sequence for the 9 internal repeats found in apoB-100 by the iterative alignment procedure (De Loof et al., 1987). The circle colors represent the residue characters: yellow, nonpolar; green, polar; red, acidic; blue, basic. The consensus sequence shows amphipathic α-helical character with a negatively charged surface exposed to the solvent.

crease in the number of lysine ϵ-amino groups. The oxidation of polyunsaturated fatty acids can form aldehydes that modify these amino groups to produce malondialdehyde and 4-hydroxynoneal (Stocker and Keaney, 2004). The lysine amino groups are also covalently modified by phospholipids (Gillotte et al., 2000). The blocking of lysine ϵ-amino groups with simultaneous fatty acid oxidation, giving hydroxyl fatty acids, generates negatively charged LDL (Gillotte et al., 2000; Stocker and Keaney, 2004). LOX-1 binds to AcLDL with comparable affinity. Acetylation blocks the lysine ϵ-amino groups without any side reactions involving lipids, thus also generating negatively charged LDL.

We propose a model involving a reduced positive charge as a possible explanation for the specific LOX-1 binding to oxidized and acetylated LDLs. Hence, the reduced surface positive charge of LDL accelerates LOX-1 binding due to a reduction of repulsive charges on the basic spine. LDL comprises the following content of charged residues: D (5.1%), E (6.5%), K (7.8%), and R (3.3%), giving an almost neutral total charge. The blocking of the ϵ-amino groups of lysine residues affects the total LDL charge, which accelerates LOX-1 binding to the surface amphipathic helices. Sequence analysis of apoB-100 has shown the presence of nine repeated amphipathic helical regions consisting of 22 residues (De Loof et al., 1987); the consensus repeating sequence is DFIDEFNEKLKDLSDQLNDFLN. The 22 residue sequence is shown as a helical wheel diagram in Figure 6B. Interestingly, this gives a negatively charged surface on the opposite side to the membrane bound hydrophobic region. The basic spine of LOX-1 must recognize the repeating helices on the LDL through electrostatic interactions. The reduced positive charge model consistently explains why AcLDL is bound by LOX-1.

Another explanation for the LOX-1-specific binding to OxLDL is the phospholipid conjugation model. Oxidized phospholipids link to lysine amino groups (Gillotte et al., 2000), and the conjugated lysine residues are then decorated with negatively charged phosphate groups. In apoB-100, there are well-defined positively charged amphipathic α helices in the β2 domain. The number of residues in the α helices are 22, 39, and 33, giving a comparable size to that of the basic spine (Segrest et al., 2001). Phospholipid conjugation to lysines in the basic helices provides the negatively charged helices recognized by the basic spine of LOX-1. This model may explain the LOX-1 binding to OxLDL, but it does not readily explain the observed AcLDL activity to LOX-1 binding.

It is difficult to evaluate the significance of the models at present, but both mechanisms may occur simultaneously to generate the modified LDL that is actively recognized by LOX-1.

Experiments with delipidated OxLDL have shown that LOX-1 recognizes modified apoB-100 in OxLDL, but cannot rule out the possibility that LOX-1 also binds to modified lipids firmly linked to apoB-100 (Moriwaki et al., 1998). Although it is generally accepted that LOX-1 recognizes the protein moiety of OxLDL, it is not yet known whether oxidized phospholipids bind to LOX-1 (Mehta, 2004). Taking into account these considerations, with the exception of apoB-100, which is

known to be cleaved in the maximally oxidized particle (Fong et al., 1987), several types of fatty acid oxidation products (Stocker and Keaney, 2004) may also contribute to the binding of LOX-1 to OxLDL by the introduction of negative charges.

Reduction in Binding Activity by Mutation at the Dimer Interface

The severe reduction in the binding activity for the W150A mutant is remarkable. We do not have any structural details on the W150A mutant, but the notable binding reduction is possibly caused by dimer disarrangement through resizing of the empty cavity in the dimer interface based on the present LOX-1 structure (Figure 5B). The ^{1}H-^{15}N two-dimensional HSQC NMR spectra for the wild-type and W150A CTLDs were compared. The similar NMR signal dispersion for the wild-type and W150A CTLDs suggests that the W150A mutant retains essentially the same CTLD fold as the wild-type (Figure S3). Therefore, the structural denaturing of W150A CTLD as a possible cause for the severe reduction in the binding activity is ruled out. This supports the idea of dimer disarrangement in W150A resulting from disruption of the basic spine structure at the dimer surface. This view also emphasizes the crucial role of the basic spine in OxLDL recognition discussed above.

Structural comparison of the ligand binding domains of crystals grown under acidic and physiological pH conditions has shown that the single binding domain does not undergo significant structural changes in response to the solution pH. However, dimer arrangement in an asymmetric unit is different under the two pH conditions. This observation might suggest dimer disarrangement of LOX-1 in endosomal pH conditions. As discussed for the W150A mutant, LOX-1 dimer disarrangement would release OxLDL in the endosome. In considering the significance of the basic spine in LOX-1 binding to OxLDL as described in the present work, endosomal pH also titrates acidic groups in apoB-100 to facilitate OxLDL release from LOX-1. By analogy with the LDL receptor, LOX-1 is also likely to be a recycling receptor. The proposed ligand-releasing mechanism is therefore important in understanding the possible recycling of LOX-1.

In summary, the crystal structure of LOX-1 presented in this paper, together with the in vivo binding analyses with several mutant proteins, demonstrates the significance of the basic spine structure on the dimer surface for OxLDL binding. Based on the consensus model of the LDL structure, several possible modes of LOX-1 binding to OxLDL are proposed. Very recently, Park and coworkers have reported the human LOX-1 crystal structure (Park et al., 2005). Their independent results are consistent with those presented in this paper. Further biochemical studies of LOX-1 recognition of OxLDL will be required to establish a complete understanding of this interaction.

Experimental Procedures

Protein Expression and Purification

Human LOX-1 cDNA used in the present work was cloned from human aortic endothelial cells (HAECs) (Shi et al., 2001). DNA encoding portions of the extracellular region of human LOX-1 were engineered for expression in *E. coli* BL21(DE3) (Stratagene, La Jolla, CA). These included the C-type lectin-like domain (CTLD; residues 143–273), the complete extracellular region (CTLD-NECK; 61–273), and the CTLD having a 14 residue NECK domain (CTLD-NECK14; 129–273). The corresponding gene fragments were cloned into pET28a (Novagen, Madison, WI) at the NdeI and XhoII sites. Proteins were expressed as inclusion bodies, denatured, refolded, and purified according to the following procedure, adapted from a similar method reported previously (Llera et al., 2001; Rudolph and Lilie, 1996).

Bacterial cells were grown in M9 minimal medium at 37°C until the culture reached an optical density at 660 nm of ~0.5. Heterologous expression was induced by the addition of isopropyl-1-thiol-β-D-galactopyranoside at 1 mM. The cells were then cultured for an additional 6 hr at 37°C before harvesting. The bacterial cells were lysed by sonication in a buffer solution containing 50 mM Tris-HCl (pH 8.0), 400 mM NaCl, 0.1% (v/v) Triton X-100. After centrifugation, the collected cell pellets containing inclusion bodies were solubilized in 6 M guanidium hydrochloride solution (pH 8.0) in 50 mM Tris-HCl, 50 mM DTT for 4 hr. Solubilized protein in the supernatant was then diluted slowly into buffer solution containing no denaturant and 50 mM Tris-HCl (pH 8.5), 0.4 M L-arginine with 5 mM reduced or 0.5 mM oxidized glutathione (GSH/GSSG mixture) as an oxide shuffling reagent. The protein in the GSH/GSSG mixture was dialyzed against a buffer solution of 25 mM Tris-HCl (pH 7.5), 50 mM NaCl, and was then concentrated on a HisTrap HP affinity column (Amersham-Pharmacia, Uppsala, Sweden). The protein was subjected to further purification by gel filtration chromatography (Superdex 75 column, Amersham-Pharmacia). The purified protein showed the anticipated binding specificity and affinity for acetylated LDL (AcLDL). This was confirmed by surface plasmon resonance (Biacore 2000, Amersham-Pharmacia) by using a sensor doped with purified LOX-1 protein.

Crystallization and Crystallography

Crystals of the LOX-1 CTLD fragment were grown from an equal volume mixture of protein solution (8.0 mg/ml protein, 10 mM Tris-HCl [pH 7.5], 50 mM NaCl) and precipitant solution (100 mM citrate [pH 3.6]) at 293 K. Crystals of the SeMet derivative of the LOX-1 CTLD were obtained by slightly modifying the above-described conditions; in brief, protein solution (7.6 mg/ml protein, 10 mM Tris-HCl [pH 7.5], 50 mM NaCl) was mixed with precipitant solution (100 mM citrate [pH 4.0–4.2]) containing 20 mM zinc acetate. The NECK14-CTLD fragment was crystallized at physiological pH from a solution made from an equal volume of protein solution (4.6 mg/ml protein, 10 mM Tris-HCl [pH 7.5], 400 mM NaCl) and precipitant solution (100 mM HEPES buffer [pH 7.5], 20% PEG 10 K [Crystal Screen 2 No.38, Hampton Research]) at 277 K.

For the SeMet derivative of the LOX-1 CTLD, diffraction data were collected at beamline BL40-B2 at Spring-8, Harima, Japan. The diffraction data were recorded on an ADSC Quantum-4 CCD scanner and processed by the HKL2000 software package (Otwinowski and Minor, 1991). Data for CTLD-NECK14 were collected at beamline BL-6B in the Photon Factory of the National Laboratory of High Energy Physics, Tsukuba, Japan. The diffraction data were recorded on a Rigaku R-AXIS IV^{2+} imaging plate detector and processed by CrystalClear (Molecular Structure Corporation) (Pflugrath, 1999). Cryocooling required that the crystals were immersed in cryoprotectant, comprising a reservoir solution plus 20% (v/v) ethylene glycol, for several seconds immediately prior to their exposure to a stream of N_2 gas at 100 K for data collection.

Phasing and Model Refinement

The structure of LOX-1 CTLD-NECK14 was determined by multiple anomalous dispersion (MAD) by using a SeMet derivative. Two selenium positions, corresponding to M202 in each subunit, were located on anomalous Patterson maps. MAD phases were calculated by using the program SHARP (de La fortelle and Bricogne, 1997). The electron density maps computed from the MAD phases allowed us to find the noncrystallographic symmetry (NCS) parameters between the two subunits within the asymmetric unit. The phases were then improved to 2.0 Å resolution by NCS averaging

by using the program DM in CCP4 (CCP4, 1998), followed by atomic model building with the program O (Jones et al., 1991). Crystallographic refinement was performed with the program CNS (Brunger et al., 1998). The crystallographic refinement and manual model correction were iterated to convergence (Table 1).

Analytical Ultracentrifugation

Sedimentation equilibrium experiments were carried out at 20°C by using a Beckman Optima XL-1 instrument. LOX-1 CTLD, CTLD-NECK14, and the whole extracellular domain were extensively dialyzed against 10 mM Tris-HCl buffer (pH 7.5) containing 50 mM NaCl (CTLD) or 400 mM NaCl (CTLD-NECK14 and the whole extracellular domain) and were concentrated to 0.1, 0.1, and 0.5 mg ml^{-1}, respectively. Equilibrium distributions were analyzed after 27 hr of centrifugation at 8,000, 15,000, and 20,000 rpm (Beckman An-50Ti rotor with double sector centerpiece), respectively. For the calculation of molecular mass, the data were fitted to an ideal single component model.

DiD-Labeled AcLDL Uptake Assays

DiD (1,1′-dioctadecyl-3,3,3′,3′-tetramethylindodicarbocyanine perchlorate)-labeled AcLDL was prepared from human LDL according to the previously described method for DiI (1,1′-dioctadecyl-3,3,3′,3′-tetramethylindocarbocyanine perchlorate) labeling (Stephan and Yurachek, 1993). CHO-K1 cells were grown on coverslips and transiently transfected with CFP-tagged native LOX-1, or mutant LOX-1s. Approximately 48 hr posttransfection, cells were incubated with DiD-AcLD for 10 min at 37°C. Excess DiD-AcLDL was removed by washing gently with fresh medium. The cells were incubated for another 10 min in order to allow for complete ligand uptake. For live cell imaging, the coverslip was then inverted onto a glass slide with a spacer. Microscopy was performed by using a Leica DM IRE2 microscope equipped with a 100×/N.A. 1.4 objective and Cool SNAP HQ-cooled CCD camera (Roper Scientific, Trenton, NJ) driven by the MetaMorph software (Universal Imaging, Downingtown, PA), under conditions that maintained cell activity. The expression level of LOX-1s was examined by CFP fluorescence by using an excitation wavelength of 436 nm (0.1 s). DiD-AcLDL uptake was analyzed by the amount of DiD-derived fluorescence excited at 620 nm (0.2 s). Examination was completed within 60 min after addition of DiD-AcLDL. Based on the observed fluorescence intensities compared with those found for the cells expressing native LOX-1, the uptake activities were assessed.

Supplemental Data

Supplemental Data including three supplemental figures are available at http://www.structure.org/cgi/content/full/13/6/905/DC1.

Acknowledgments

The authors declare that they have no competing financial interests. This work was supported by the Japan New Energy and Industrial Technology Development Organization (NEDO).

Received: February 10, 2005
Revised: March 27, 2005
Accepted: March 27, 2005
Published: June 7, 2005

References

Aoyama, T., Sawamura, T., Furutani, Y., Matsuoka, R., Yoshida, M.C., Fujiwara, H., and Masaki, T. (1999). Structure and chromosomal assignment of the human lectin-like oxidized low-density-lipoprotein receptor-1 (LOX-1) gene. Biochem. J. *339*, 177–184.

Brunger, A.T., Adams, P.D., Clore, G.M., DeLano, W.L., Gros, P., Grosse-Kunstleve, R.W., Jiang, J.S., Kuszewski, J., Nilges, M., Pannu, N.S., et al. (1998). Crystallography & NMR system: a new software suite for macromolecular structure determination. Acta Crystallogr. D Biol. Crystallogr. *54*, 905–921.

CCP4 (Collaborative Computational Project, Number 4) (1998). The CCP4 suite: programs for protein crystallography. Acta Crystallogr. D Biol. Crystallogr. *50*, 760–763.

Chen, M., Kakutani, M., Minami, M., Kataoka, H., Kume, N., Narumiya, S., Kita, T., Masaki, T., and Sawamura, T. (2000). Increased expression of lectin-like oxidized low density lipoprotein receptor-1 in initial atherosclerotic lesions of Watanabe heritable hyperlipidemic rabbits. Arterioscler. Thromb. Vasc. Biol. *20*, 1107–1115.

Chen, M., Inoue, K., Narumiya, S., Masaki, T., and Sawamura, T. (2001). Requirements of basic amino acid residues within the lectin-like domain of LOX-1 for the binding of oxidized low-density lipoprotein. FEBS Lett. *499*, 215–219.

Chen, M., Masaki, T., and Sawamura, T. (2002). LOX-1, the receptor for oxidized low-density lipoprotein identified from endothelial cells: implications in endothelial dysfunction and atherosclerosis. Pharmacol. Ther. *95*, 89–100.

de La fortelle, E., and Bricogne, G. (1997). Maximum-likelihood heavy-atom parameter refinement in the MIR and MAD methods. Methods Enzymol. *276*, 472–494.

De Loof, H., Rosseneu, M., Yang, C.Y., Li, W.H., Gotto, A.M., and Chan, L. (1987). Human apolipoprotein B: analysis of internal repeats and homology with other apolipoproteins. J. Lipid Res. *28*, 1455–1465.

Doi, T., Higashino, K., Kurihara, Y., Wada, Y., Miyazaki, T., Nakamura, H., Uesugi, S., Imanishi, T., Kawabe, Y., and Itakura, H. (1993). Charged collagen structure mediates the recognition of negatively charged macromolecules by macrophage scavenger receptors. J. Biol. Chem. *268*, 2126–2133.

Drickamer, K. (1999). C-type lectin-like domains. Curr. Opin. Struct. Biol. *9*, 585–590.

Fong, L.G., Parthasarathy, S., Witztum, J.L., and Steinberg, D. (1987). Nonenzymatic oxidative cleavage of peptide bonds in apoprotein B-100. J. Lipid Res. *28*, 1466–1477.

Gillotte, K.L., Horkko, S., Witztum, J.L., and Steinberg, D. (2000). Oxidized phospholipids, linked to apolipoprotein B of oxidized LDL, are ligands for macrophage scavenger receptors. J. Lipid Res. *41*, 824–833.

Jones, T.A., Zou, J.Y., and Cowan, S.W. (1991). Improved methods for building protein models in electron density maps and the location of errors in these models. Acta Crystallogr A *47 (Pt 2)*, 110–119.

Kataoka, H., Kume, N., Miyamoto, S., Minami, M., Moriwaki, H., Murase, T., Sawamura, T., Masaki, T., Hashimoto, N., and Kita, T. (1999). Expression of lectinlike oxidized low-density lipoprotein receptor-1 in human atherosclerotic lesions. Circulation *99*, 3110–3117.

Kita, T. (1999). LOX-1, a possible clue to the missing link between hypertension and atherogenesis. Circ. Res. *84*, 1113–1115.

Kita, T., Kume, N., Minami, M., Hayashida, K., Murayama, T., Sano, H., Moriwaki, H., Kataoka, H., Nishi, E., Horiuchi, H., et al. (2001). Role of oxidized LDL in atherosclerosis. Ann. N Y Acad. Sci. *947*, 199–206.

Koradi, R., Billeter, M., and Wuthrich, K. (1996). MOLMOL: a program for display and analysis of macromolecular structures. J. Mol. Graph. *14*, 51–55.

Kraulis, P.J. (1991). MOLSCRIPT: a program to produce both detailed and schematic plots of protein structures. J. Appl. Crystallogr. *24*, 946–950.

Li, D., and Mehta, J.L. (2000). Upregulation of endothelial receptor for oxidized LDL (LOX-1) by oxidized LDL and implications in apoptosis of human coronary artery endothelial cells: evidence from use of antisense LOX-1 mRNA and chemical inhibitors. Arterioscler. Thromb. Vasc. Biol. *20*, 1116–1122.

Li, D., Yang, B., and Mehta, J.L. (1998). Ox-LDL induces apoptosis in human coronary artery endothelial cells: role of PKC, PTK, bcl-2, and Fas. Am. J. Physiol. *275*, H568–H576.

Li, P., Morris, D.L., Willcox, B.E., Steinle, A., Spies, T., and Strong, R.K. (2001). Complex structure of the activating immunoreceptor NKG2D and its MHC class I-like ligand MICA. Nat. Immunol. *2*, 443–451.

Li, D., Chen, H., Romeo, F., Sawamura, T., Saldeen, T., and Mehta, J.L. (2002a). Statins modulate oxidized low-density lipoprotein-mediated adhesion molecule expression in human coronary artery endothelial cells: role of LOX-1. J. Pharmacol. Exp. Ther. *302*, 601–605.

Li, P., McDermott, G., and Strong, R.K. (2002b). Crystal structures of RAE-1beta and its complex with the activating immunoreceptor NKG2D. Immunity *16*, 77–86.

Llera, A.S., Viedma, F., Sanchez-Madrid, F., and Tormo, J. (2001). Crystal structure of the C-type lectin-like domain from the human hematopoietic cell receptor CD69. J. Biol. Chem. *276*, 7312–7319.

Lougheed, M., and Steinbrecher, U.P. (1996). Mechanism of uptake of copper-oxidized low density lipoprotein in macrophages is dependent on its extent of oxidation. J. Biol. Chem. *271*, 11798–11805.

Lupas, A. (1996). Coiled coils: new structures and new functions. Trends Biochem. Sci. *21*, 375–382.

McFarland, B.J., Kortemme, T., Yu, S.F., Baker, D., and Strong, R.K. (2003). Symmetry recognizing asymmetry: analysis of the interactions between the C-type lectin-like immunoreceptor NKG2D and MHC class I-like ligands. Structure *11*, 411–422.

Mehta, J.L. (2004). The role of LOX-1, a novel lectin-like receptor for oxidized low density lipoprotein, in atherosclerosis. Can. J. Cardiol. *20* (Suppl B), 32B–36B.

Mehta, J.L., Li, D.Y., Chen, H.J., Joseph, J., and Romeo, F. (2001). Inhibition of LOX-1 by statins may relate to upregulation of eNOS. Biochem. Biophys. Res. Commun. *289*, 857–861.

Moriwaki, H., Kume, N., Sawamura, T., Aoyama, T., Hoshikawa, H., Ochi, H., Nishi, E., Masaki, T., and Kita, T. (1998). Ligand specificity of LOX-1, a novel endothelial receptor for oxidized low density lipoprotein. Arterioscler. Thromb. Vasc. Biol. *18*, 1541–1547.

Murase, T., Kume, N., Kataoka, H., Minami, M., Sawamura, T., Masaki, T., and Kita, T. (2000). Identification of soluble forms of lectin-like oxidized LDL receptor-1. Arterioscler. Thromb. Vasc. Biol. *20*, 715–720.

Murphy, R.F., Powers, S., and Cantor, C.R. (1984). Endosome pH measured in single cells by dual fluorescence flow cytometry: rapid acidification of insulin to pH 6. J. Cell Biol. *98*, 1757–1762.

Nagase, M., Hirose, S., Sawamura, T., Masaki, T., and Fujita, T. (1997). Enhanced expression of endothelial oxidized low-density lipoprotein receptor (LOX-1) in hypertensive rats. Biochem. Biophys. Res. Commun. *237*, 496–498.

Natarajan, K., Dimasi, N., Wang, J., Mariuzza, R.A., and Margulies, D.H. (2002). Structure and function of natural killer cell receptors: multiple molecular solutions to self, nonself discrimination. Annu. Rev. Immunol. *20*, 853–885.

Nicholls, A., Sharp, K.A., and Honig, B. (1991). Protein folding and association: insights from the interfacial and thermodynamic properties of hydrocarbons. Proteins *11*, 281–296.

Otwinowski, Z., and Minor, W. (1991). Processing of X-ray diffraction data collected in oscillation mode. Methods Enzymol. *276*, 307–326.

Park, H., Adsit, F.G., and Boyington, J.C. (2005). The 1.4 Å crystal structure of the human oxidized low-density lipoprotein LOX-1. J. Biol. Chem. *280*, 13593–13599.

Pflugrath, J.W. (1999). The finer things in X-ray diffraction data collection. Acta Crystallogr. D Biol. Crystallogr. *55*, 1718–1725.

Radaev, S., Rostro, B., Brooks, A.G., Colonna, M., and Sun, P.D. (2001). Conformational plasticity revealed by the cocrystal structure of NKG2D and its class I MHC-like ligand ULBP3. Immunity *15*, 1039–1049.

Rudenko, G., Henry, L., Henderson, K., Ichtchenko, K., Brown, M.S., Goldstein, J.L., and Deisenhofer, J. (2002). Structure of the LDL receptor extracellular domain at endosomal pH. Science *298*, 2353–2358.

Rudolph, R., and Lilie, H. (1996). In vitro folding of inclusion body proteins. FASEB J. *10*, 49–56.

Sawamura, T., Kume, N., Aoyama, T., Moriwaki, H., Hoshikawa, H., Aiba, Y., Tanaka, T., Miwa, S., Katsura, Y., Kita, T., and Masaki, T. (1997). An endothelial receptor for oxidized low-density lipoprotein. Nature *386*, 73–77.

Segrest, J.P., Jones, M.K., De Loof, H., and Dashti, N. (2001). Structure of apolipoprotein B-100 in low density lipoproteins. J. Lipid Res. *42*, 1346–1367.

Shi, X., Niimi, S., Ohtani, T., and Machida, S. (2001). Characterization of residues and sequences of the carbohydrate recognition domain required for cell surface localization and ligand binding of human lectin-like oxidized LDL receptor. J. Cell Sci. *114*, 1273–1282.

Steinbrecher, U.P. (1999). Receptors for oxidized low density lipoprotein. Biochim. Biophys. Acta *1436*, 279–298.

Stephan, Z.F., and Yurachek, E.C. (1993). Rapid fluorometric assay of LDL receptor activity by DiI-labeled LDL. J. Lipid Res. *34*, 325–330.

Stocker, R., and Keaney, J.F., Jr. (2004). Role of oxidative modifications in atherosclerosis. Physiol. Rev. *84*, 1381–1478.

Tormo, J., Natarajan, K., Margulies, D.H., and Mariuzza, R.A. (1999). Crystal structure of a lectin-like natural killer cell receptor bound to its MHC class I ligand. Nature *402*, 623–631.

Weis, W.I., Kahn, R., Fourme, R., Drickamer, K., and Hendrickson, W.A. (1991). Structure of the calcium-dependent lectin domain from a rat mannose-binding protein determined by MAD phasing. Science *254*, 1608–1615.

Weis, W.I., Drickamer, K., and Hendrickson, W.A. (1992). Structure of a C-type mannose-binding protein complexed with an oligosaccharide. Nature *360*, 127–134.

Xie, Q., Matsunaga, S., Niimi, S., Ogawa, S., Tokuyasu, K., Sakakibara, Y., and Machida, S. (2004). Human lectin-like oxidized low-density lipoprotein receptor-1 functions as a dimer in living cells. DNA Cell Biol. *23*, 111–117.

Yokoyama, W.M., and Plougastel, B.F. (2003). Immune functions encoded by the natural killer gene complex. Nat. Rev. Immunol. *3*, 304–316.

Yoshida, H., Kondratenko, N., Green, S., Steinberg, D., and Quehenberger, O. (1998). Identification of the lectin-like receptor for oxidized low-density lipoprotein in human macrophages and its potential role as a scavenger receptor. Biochem. J. *334*, 9–13.

Zelensky, A.N., and Gready, J.E. (2003). Comparative analysis of structural properties of the C-type-lectin-like domain (CTLD). Proteins *52*, 466–477.

Accession Numbers

The coordinates of the crystal structure of human LOX-1 at low pH and the crystal structure of the human LOX-1 disulfide-linked dimer have been deposited in the Protein Data Bank under codes 1YXJ and 1YXK, respectively.